Photosynthesis Research **51:** 193–208, 1997.

Regular paper

Photosynthetic oxygen evolution: H/D isotope effects and the coupling between electron and proton transfer during the redox reactions at the oxidizing side of Photosystem II

Michael Haumann, Oliver Bögershausen, Dmitry Cherepanov[1], Ralf Ahlbrink & Wolfgang Junge*

*Abteilung Biophysik, FB. Biologie/ Chemie, Barbarastr. 11, Universität Osnabrück, D-49069 Osnabrück, Germany; [1]Institute of Electrochemisty, Russian Academy of Sciences, Leninskii Prospect 31, 117071 Moscow, Russia; *Author for correspondence.*

Received 12 November 1996; accepted in revised form 23 January 1997

Key words: electron transfer, H/D-isotope effect, peroxide, photosystem II, proton release, water oxidation

Abstract

The oxygen evolving complex (OEC) of Photosystem II (PS II) incorporates a Mn-cluster and probably a further redox cofactor, X. Four quanta of light drive the OEC through the increasingly oxidized states $S_0 \Rightarrow S_1 \Rightarrow S_2 \Rightarrow S_3 \Rightarrow S_4$ to yield O_2 during the transition $S_4 \rightarrow S_0$. It has been speculated that the oxidation of water might be kinetically facilitated by the abstraction of hydrogen. This implied that the respective electron acceptor is deprotonated upon oxidation. Whether Y_Z and X fulfill this expectation is under debate. We have previously inferred a 'chemical' deprotonation of X based on the kinetics of proton release (Haumann M, Drerenstedt W, Hundelt M and Junge W (1996) Biochim Biophys Acta 1273: 237–250. Here, we investigated the rates of electron transfer and proton release as function of the D_2O/H_2O ratio, the pH, and the temperature both in thylakoids and PS II core particles. The largest kinetic isotope effect on the rate of electron transfer (factor of 2.1–2.4) and the largest pH-dependence (factor of about 2 between pH 5 and 8) was found on $S_2 \Rightarrow S_3$ where X is oxidized. During the other transitions both factors were much smaller (≤ 1.4). Electron transfer is probably kinetically steered by proton transfer only during $S_2 \Rightarrow S_3$. These results corroborate the notion that $X^{\bullet}$ serves as a hydrogen acceptor for bound water during $S_4 \rightarrow S_0$. We propose a consistent scheme for the final reaction with water to yield dioxygen: two two-electron (hydrogen) transfers in series with a peroxide intermediate.

Abbreviations: BSA – bovine serum albumin; DCBQ – 2,5-dichloro-*p*-benzoquinone; DNP-INT – dinitrophenylether of iodonitrothymol; EPR – electron paramagnetic resonance; FWHM – full width at half maximum; His – histidine; Mes – 2-N-morpholinoethane sulfonic acid; Mn – manganese; P_{680} – primary donor; OEC – oxygen evolving complex = Mn_4X-entity; PS II – Photosystem II; Q_A – primary quinone acceptor; UV – ultra violet; Y_Z – D1-tyrosine-161; X – redox cofactor

Introduction

Photosystem II (PS II) of cyanobacteria and green plants uses water as the terminal electron donor. Each absorbed quantum of light induces a charge separation yielding the charge pair P_{680}^+ and Q_A^-. P_{680}^+ is reduced by Y_Z (Tyr-161 on subunit D1) in nanoseconds. Y_Z^{ox} stepwise oxidizes the other redox cofactors of the oxygen evolving complex (OEC) during the four transitions from state S_0 to S_4. S_4 spontaneously decays into S_0 under release of dioxygen. It has been argued that water oxidation is kinetically and thermodynamically facilitated by a concerted electron/proton transfer to avoid electrostatic complications (Krishta-

lik 1990; Haumann and Junge 1994; Hoganson et al. 1995, Gilchrist et al. 1995; Britt 1996). It is widely agreed on that the Mn-cluster itself is oxidized on transitions $S_0 \Rightarrow S_1$ and $S_1 \Rightarrow S_2$ (Debus 1992; Brudvig 1995; Britt 1996). On transition $S_2 \Rightarrow S_3$ the oxidized species is probably not Mn as evident from X-ray (Klein et al. 1993; Roelofs et al. 1996) and EPR spectroscopy (Kusunoki 1995) although there have been conflicting reports (Ono et al. 1992, 1995). The tentative identification of this component, named X in the following, with histidine (His) has been based on EPR-, FTIR- and UV-spectroscopy. In these studies Ca^{2+}-(Boussac et al. 1990; Berthomieu and Boussac 1995), Mn- (Allakhverdiev et al. 1992; Ono and Inoue 1991) and Cl^--depleted material (Boussac and Rutherford 1994; Haumann et al. 1996) has been used. In Cl^--depleted dark-adapted PS II core particles X^{ox} and $Y_Z{}^{ox}$ were consecutively and stably formed on the first two flashes (Haumann et al. 1996). $Y_Z{}^{ox}$ formation on the second flash was compatible with the observation of the so-called split EPR signal at $g \approx 2$ on this flash in BBY-membranes (Boussac and Rutherford 1994) which has recently been attributed to a tyrosine radical from pulsed EPR experiments (Tang et al. 1996a). We previously investigated the rate of deprotonation at the oxidizing side of PS II. The dependence of this rate on the concentration of the pH-indicator (Haumann and Junge 1994) and on the pH (Bögershausen and Junge 1995a,b) allowed to discriminate proton release by peripheral anmino acids (electrostatic release) against proton release by redox cofactors (chemical release) (see (Haumann and Junge 1996) for review). In a study aiming particularly at the transition $S_2 \Rightarrow S_3$ we found a component of proton release that was kinetically coupled to electron transfer and thus resulted from the respective cofactor, X, itself (Haumann et al. 1995, 1996). This attribution was compatible with known data on local electrochromism. Peripheral proton release does not elicit an electrochromic response of intrinsic pigments (Haumann et al. 1994). Long-lived electrochromic absorption transients, which are indicative of *uncompensated charges in the catalytic center*, are only observed during $S_1 \Rightarrow S_2$ but not during $S_0 \Rightarrow S_1$ and $S_2 \Rightarrow S_3$ (Saygin and Witt 1987; Haumann et al. 1994). This observation favours the deprotonation of a redox cofactor during $S_2 \Rightarrow S_3$ (and possibly also during $S_0 \Rightarrow S_1$, but see farther down).

The evidence for X^{ox} being deprotonated and thus electroneutral is in conflict with the following statements as put forward by other authors: (1) The stepwise decrease of the rate of electron transfer from the OEC to $Y_Z{}^{ox}$ when progressing from $S_0 \Rightarrow S_1$ to $S_3 \Rightarrow S_4 \rightarrow S_0$ reflects the coulombic effect of the successive deposition of four electrostatically *uncompensated* positive charges on Mn (Dekker et al. 1984). (2) The absence of electrochromic transients during $S_0 \Rightarrow S_1$ and $S_2 \Rightarrow S_3$ is indicative of the deprotonation of bound water (Saygin and Witt 1987). (3) Y_Z, which is transiently oxidized during all steps, acts as a hydrogen atom abstractor from water on every of the four transitions $S_0 \Rightarrow S_1$ to $S_3 \Rightarrow S_4$, and stable electrochromic transients on $S_1 \Rightarrow S_2$ are caused by the redistribution of bound Cl^- in the OEC (Babcock 1995; Hoganson et al. 1995).

These conflicting statements prompted us to investigate the interplay between proton (hydrogen) and electron transfer from another viewpoint, mainly by kinetic isotope effects. Previous reports on kinetic H/D isotope effects on the rate of electron transfer $OEC \rightarrow Y_Z{}^{ox}$ have produced conflicting results: On $S_1 \Rightarrow S_2$ a ratio k_H/k_D of 1.3 was obtained by UV-spectroscopy (Renger et al. 1994). It contrasted with a ratio of 2.9 by EPR (Lydakis-Simantiris et al. 1995). On $S_2 \Rightarrow S_3$ a ratio of 1.1–1.3 was observed in the two former studies but of about 2 in more recent work (Karge et al. 1996).

We reevaluated this matter at a wider scale by studying, in parallel, the rates of oxygen evolution by a kinetically competent Clark-type electrode, the rate of electron transfer to $Y_Z{}^{ox}$ by UV-spectroscopy, and the rate of proton release by pH-indicating dyes. We varied the H/D-isotopic ratio, the pH and the temperature.

Materials and methods

Unstacked thylakoids and PS II core particles were prepared from pea seedlings as in (Haumann and Junge 1994) and (Bögershausen and Junge 1995b, modified after van Leeuwen et al. 1991). The preparations were stored at $-80°C$ until use and, after thawing, suspended at 40 μM of chlorophyll in a medium with 10 mM NaCl, 2.6 g/l BSA and 10 μM DNP-INT (thylakoids) and 5 μM chlorophyll, 10 mM $CaCl_2$ and 10 mM MES-buffer (core particles). MES was omitted in experiments on pH-transients with core particles. Further conditions are indicated in the figure legends.

Inactivation of core particles was performed by titrating a suspension of 50 μM of chl. to pH 9 for 5 min and then back to the desired pH for the measurements. After this treatment the rate of oxygen evolution under continuous light was below 10% of a control.

Flash-spectrophotometry (Junge 1976) was performed at a digitizing time per address of 10 μs with a Q-switched Ruby-laser (694 nm, FWHM 50 ns) and a Xenon-flash lamp (>610 nm, FWHM 10 μs) as excitation sources. With thylakoids every train of flashes was recorded with a fresh sample, which was filled into the cuvette (optical path 1 cm) from a light shielded reservoir. With core particles we used repetitive dark-adaptation (Bögershausen and Junge 1995b) with a flash train spacing of 20 s and not more than 50 recordings per sample. Up to 500 transients were digitized and averaged on a Nicolet Pro30 recorder to improve the signal-to-noise ratio. *The rates of the oxidoreduction of the OEC* were determined from flash-induced UV-absorption transients of the manganese/X-entity at 360 nm (Renger and Hanssum 1992) and by local electrochromism at the wavelength difference 443–424 nm. Transients at 424 nm were subtracted from the ones at 443 nm to remove all contributions from the acceptor side of PS II (Haumann et al. 1994, 1996; Rappaport et al. 1994). The resulting difference was solely due to events at its oxidizing side. *Proton release* was measured at high time resolution with the pH-indicating dyes neutral red (20 μM) at 548 nm with thylakoids (Haumann and Junge 1994) and bromocresol purple (30 μM) at 575 nm with core particles (Bögershausen and Junge 1995b). From transients in the presence of dye background transients obtained without the dye were subtracted (± dye). *The oxidoreduction of* $P_{680}{}^{+}$ was time resolved at 820 nm with an upper time per address of 2 ns (analogue bandwidth 1 GHz). We used the same setup, namely a 820 nm diode-laser as measuring light source, and a Nd:YAG-laser for flash excitation (FWHM 6 ns, 532 nm) as previously described (Haumann et al. 1996).

Oxygen evolution on the third flash in a row was time resolved at 50 μs per address by a home-built centrifugable Clark-type electrode. 20 μl of a PS II containing suspension were pelleted on its bare platinum surface by centrifugation (20 min in darkness, 20 °C, swing out rotor, Beckmann TJ6 centrifuge, 3000 rpm). After connecting the electrode to a current-to-voltage amplifier (home-built) and an additional dark-adaptation of 5 min, saturating Xenon flashes (>610 nm, spacing 100 ms) were provided through a light guide and the resulting signals were digitized at 50 μs per address by a Nicolet Pro10 recorder. The polarization voltage of –650 mV was applied to the platinum two minutes before the measurements.

The substitution of D_2O for H_2O was performed as follows: after thawing, the PS II containing material was suspended in a medium with the desired H_2O/D_2O ratio (D_2O was 99.7% pure, kindly provided by Prof. K. Ibel, Grenoble/Osnabrück) at pL = 6.5 (L = lyonium ion, H or D) and at the final chlorophyll concentrations for the measurements. Samples were then incubated in the light (2 mW cm^{-2}) for 5 min and, after readjusting the pL to the desired value, the samples were dark-adapted for 15 min prior to the first flash train. *The temperature of samples* was maintained by a themostated bath (Colora WK1) which was connected to a water-jacketed cuvette holder (home-built). It was measured in the cuvette by a PT100 element. The temperature was stable within ± 1 °C.

Table 1. Comparison of the half-rise times of electron transfer at the OEC in thylakoids and oxygen evolving PS II core particles. UV-transients: data from transients at 360 nm, oxygen evolution: from time resolved O_2-measurements, proton release: from a double flash experiment (see text)

Transition	Observable	Thylakoids	Core particles
		$t_{1/2}$ of electron transfer, μs	
$S_0 \Rightarrow S_1$	UV-transients	50	60
$S_1 \Rightarrow S_2$		65	80
$S_2 \Rightarrow S_3$		245	260
$S_4 \rightarrow S_0$		1300	4600
	Oxygen evolution	1600	5000
	Proton release	1300	4700

Results

A comparison of the rates of electron transfer in thylakoids and PS II core particles

Absorption transients at 360 nm were recorded on flash numbers 1 to 4 as applied to dark-adapted thylakoids and core particles (H_2O, pH 6.5). Original transients obtained on flash no. 3 in a row are given in Figure 1, top. For further examples on flashes 1, 2, and 4 see Figure 3. Rising components after flashes 4, 1 and 2 (Figure 3) and a decay after flash no. 3 (Figure 1, top) were attributed to the electron transfer at the OEC on transitions $S_0 \Rightarrow S_1$, $S_1 \Rightarrow S_2$, $S_2 \Rightarrow S_3$, and $S_4 \rightarrow S_0$ as previously (Dekker et al. 1984; Renger and Hanssum 1992; Haumann et al. 1994). The half-live times of *the oxidation of the OEC* on transitions $S_0 \Rightarrow S_1$, $S_1 \Rightarrow S_2$, and $S_2 \Rightarrow S_3$ were about the same in both materials (summarized in Table 1) and in line with the literature (Dekker et al. 1984; Renger and Hanssum 1992; van Leeuwen et al. 1992) except for one conflicting

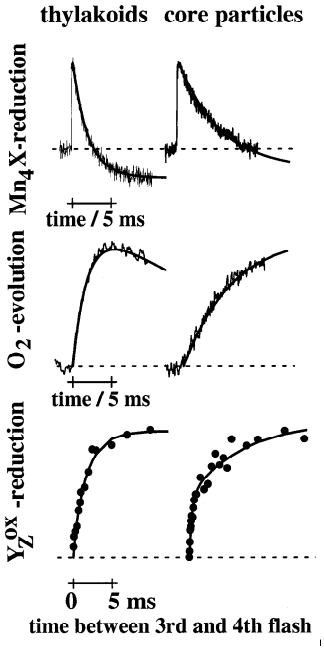

Figure 1. Transients indicating OEC-reduction, O_2-evolution and Y_Z^{ox}-reduction in dark-adapted thylakoids (left) and core particles (right). UV absorption transients on the third flash at 360 nm represent the oxidoreduction of Mn_4X of the OEC (upper traces, 100 transients averaged), O_2-evolution on the third flash is shown in the middle traces (single shot transient). The bottom traces show the extents of proton release on a fourth flash given at time intervalls ranging from 40 μs to 20 ms after three priming flashes. Proton release was monitored with the dyes neutral red (thylakoids) and bromocresol purple (core particles). For some raw transients see (Haumann and Junge 1994; Bögershausen and Junge 1995). The smooth lines were calculated with half-risetimes and relative extents of 1.3 ms (75%) and 150 μs (25%) in thylakoids (left) and of 4.7 ms (60%) and 150 μs (40%) in core particles (right). The ms-components resulted from transition $S_4 \rightarrow S_0$ (Table 1), the minor μs-components from the lower S-transitions due to the probability of misses. UV-transients were recorded with 200 μM DCBQ, proton release with 200 μM DCBQ plus 3 mM hexacyanoferrate(III) as electron acceptors and with flash intervals of 1 s (thylakoids) and 100 ms (core particles). Under these conditions Q_A^- was rapidly oxidized after the third flash (100 μs, (Lübbers et al. 1993)). No external electron acceptor was present in the O_2 measurements with thylakoids, 10 μM DCBQ were used with core particles. The pH was 6.5.

report (Rappaport et al. 1994). They were also similar to the ones obtained with core particles (Haumann et al. 1996) prepared according to another protocol (Ghanotakis et al. 1987; Lübbers et al. 1993). Minor variations were attributable to the probability of misses. On the third flash (Figure 1, top), which oxidized Y_Z and thereby induced *the reduction of the OEC by electrons from bound water* during $S_4 \rightarrow S_0$, the half-time of the latter greatly differed between thylakoids (1.3 ms) and core particles (4.6 ms, see Table 1). About the same time constants were consistently obtained (Table 1) from transients of *oxygen release* as recorded with the kinetically competent electrode (Figure 1, middle). *The reduction of Y_Z^{ox} on $S_4 \rightarrow S_0$* was independently resolved by a pump-probe technique with three flashes fired at a fixed spacing and a forth one fired at a variable interval after the third (40 μs to 20 ms). The extent of proton release caused by a fourth flash after three priming flashes given to dark-adapted samples was taken as indicative of the recovery of Y_Z (for further details see the legend of Figure 1). As documented in Figure 1 (bottom) the major portion of proton release by the forth flash appeared with similar time constant as obtained from UV-transients and oxygen evolution (Table 1) both in thylakoids (left, 1.3 ms, 75%) and in core particles (right, 4.7 ms, 60%). Minor portions were attributable to other transitions according to the given Kok-parameters.

A large effect of the type of preparation on the reaction rate was only observed for the oxygen evolving step, $S_4 \rightarrow S_0$. That it was likewise apparent in recordings of oxygen release and of the reduction of Y_Z^{ox} corroborated that the latter was limited by the catalytic event. This is in line with published evidence obtained by optical (Renger and Weiss 1986), EPR (Babcock et al. 1976) and polarographic techniques (Bouges-Bocquet 1973; Sinclair and Arnason 1974). Not unexpectedly, the final reaction with bound water was most sensitive to structural alterations. The electron transfer between Mn_4, X (His), Y_Z, and P_{680}, on the other hand, was much less affected by structural alterations.

H/D-isotope effects upon the electron transfer steps OEC$\rightarrow Y_Z \rightarrow P_{680}$

Samples of thylakoids and core particles were prepared and incubated in H_2O and D_2O as outlined under 'Materials and methods'. UV-transients at 360 nm were measured with dark-adapted material (see Figure 3 for examples of raw data). The signal extents were almost equal (deviation $\pm$ 5%) in H_2O and D_2O. We calculated the Kok-parameters from the patterns of the extent of the millisecond components (Table 1) as function of the flash number as depicted in Figure 2 (solid circles, H_2O; open circles, D_2O). The relative amounts of misses (α), double hits (β) and the fractions of centers initially in states S_0 and S_1 were determined as previously (Lübbers et al. 1993). In thylakoids the patterns were well described with (α, β, S_0): 9%, 8.5%, 5% in H_2O and 14%, 6.5%, 10% in D_2O (Figure 2, solid and dashed lines). In core particles we obtained: 20%, 6%,

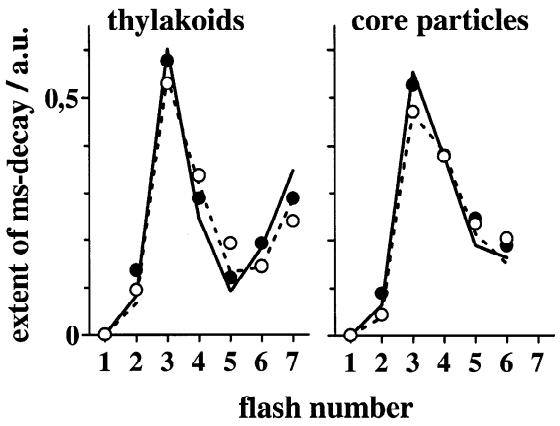

Figure 2. The pattern of O_2-release is only weakly affected by H/D-exchange. The extent of the component with $t_{1/2}$ of 1.3 ms (thylakoids) and 4.6 ms (core particles) from UV-transients at 360 nm as function of the flash number was taken as indicative for the amount of centers undergoing $S_3 \Rightarrow S_4 \rightarrow S_0$. Solid circles: H_2O, open circles: D_2O. The lines were calculated with the Kok-parameters as given in the text.

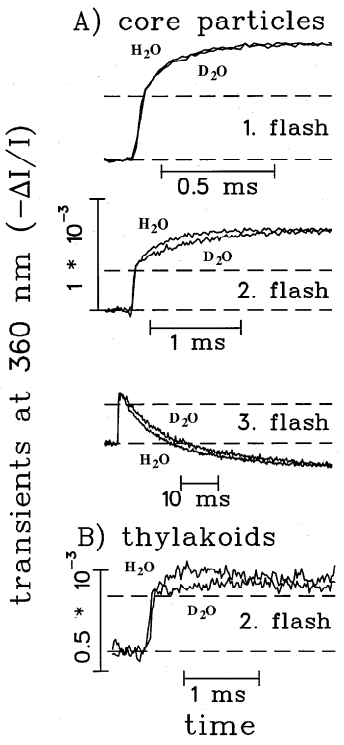

Figure 3. Electron transfer as function of the H/D ratio. (A) Absorption transients at 360 nm induced by the first 3 flashes (top to bottom) in dark-adapted core particles in H_2O and D_2O. The dashed lines indicate the extent of the jump attributable to the reduction of Q_A in < 1 ns (here slurred by the electrical bandwidth setting). Time resolution 20 μs per address, 500 transients were averaged, excitation by a Xenon-lamp, 8 μM of chlorophyll, 100 μM DCBQ served as electron acceptor. Note the different time scales of the three transients. (B) The transients on flash no. 2 in dark- adapted thylakoids in H_2O and D_2O. Time resolution 20 μs per address, 200 transients averaged, Xenon-flash, 30 μM of chlorophyll, 300 μM DCBQ plus 2 mM hexacyanoferrate(III).

12% in H_2O and 20%, 4%, 15% in D_2O. These parameters were in line with our previous data (Haumann and Junge 1994; Bögershausen and Junge 1995b). They showed that the centers were well synchronized both in H_2O and D_2O. The greater miss factor in core particles reflected their reduced antenna size (Haumann et al. 1994). A slightly increased probability of misses and/or a larger portion of S_0 in the dark was observed in D_2O. These differences were, however, rather small and are neglected in the following.

Figure 3A shows transients at 360 nm on the first three flashes in dark-adapted PS II core particles in H_2O and D_2O (18 °C, pH 6.3). Each flash induced a jump (dashed lines) due to the reduction of Q_A (Velthuys 1988) in < 1 ns (Trissl et al. 1987). The slower rises on flashes 1 and 2 (Figure 3A) and on flash no. 4 (not shown) were attributable to the oxidation of the OEC by Y_Z^{ox} on transitions $S_1 \Rightarrow S_2$ and $S_2 \Rightarrow S_3$, and $S_0 \Rightarrow S_1$ (Dekker et al. 1984; van Leeuwen et al. 1992). On flashes 4 and 1 the time course was only slightly altered in D_2O. The ratio of k_{H2O}/k_{D2O} was 1.3 (Table 2). On flash no. 2, mainly inducing $S_2 \Rightarrow S_3$, the kinetic isotope effect was larger, namely 2.1. Its magnitude was independent of the incubation time in D_2O ranging between 10 minutes and two hours. This result indicated that the exchange of D_2O for H_2O was rapid. The decay on flash no. 3 due to transition $S_4 \rightarrow S_0$ (Figure 3A) revealed a smaller kinetic isotope effect of 1.4 (Table 2). We evaluated the kinetic isotope effect on the first two flashes in thylakoids (pH 7.4, 18 °C). On flash no. 1 (data not shown) which mainly induced $S_1 \Rightarrow S_2$ substitution of H_2O for D_2O decreased the rate of electron transfer only by a factor of about 1.2 ($t_{1/2}$ = 60 vs. 75 μs, Table 2). On flash no. 2 (Figure 3B, mainly $S_2 \Rightarrow S_3$) the kinetic isotope effect was larger, namely 2.4 ($t_{1/2}$ = 150 vs. 360 μs, Table 2). These results showed that the kinetic isotope effects were similar in thylakoids and core particles.

The rates of electron transfer at the OEC were determined from transients at 360 nm as function of the temperature (between 3 and 34 °C). They were plotted in Figure 4A according to the Arrhenius equation

$$\ln k = \ln A_0 - E_a/RT \qquad (1)$$

The rates on transition $S_1 \Rightarrow S_2$ (triangles) implied an activation energy (E_a) of 14.6 kJ/mol (dashed lines, both in H_2O, full symbols, and in D_2O, open symbols). The preexponential factors, ln A_0, were 15.0 in H_2O and 14.8 in D_2O. The ratio k_{H2O}/k_{D2O} of $\approx$1.3 was about independent of the temperature. On $S_2 \Rightarrow S_3$ (circles) the activation energy was by 10 kJ/mol larger in D_2O than in H_2O (35 kJ/mol vs. 45 kJ/mol). The ratio k_{H2O}/k_{D2O} decreased from 2.4 at 5 °C to 1.4 at 35 °C. The straight lines drawn through the experimental points (Figure 4A) intersected with each other at higher temperatures and with the coordinate at values of ln A_0 of 22.1 (H_2O) and 25.7 (D_2O). The rates of the O_2-evolving step $S_4 \Rightarrow S_0$ (squares) revealed an activation energy of about 37.5 $\pm$2 kJ/mol both in H_2O and D_2O (dotted lines). The activation energies and the preexponential factors are summarized in Table 3.

We checked these results by monitoring, in H_2O and D_2O, the decay of local electrochromism at 443-424 nm which is caused by the reduction of Y_Z^{ox} by electrons from the OEC (Rappaport et al. 1994; Haumann et al. 1996). The rates on transition $S_2 \Rightarrow S_3$ were slightly higher (Figure 4A, stars) than the ones determined at a wavelength of 360 nm, but the kinetic isotope effects were similar. The latter held true for the other transitions as well.

In general, the preexponential (frequency) factor (A_0) of the Arrhenius equation (1) is diagnostic of the nature of the rate limiting process: The frequency of molecular vibrations is about 10^{12} s^{-1} whereas the frequency of electron coupling should be some orders of magnitude lower. (1) In the case of $S_1 \Rightarrow S_2$ A_0 was about $3 \cdot 10^6$ s^{-1}. Taking the kinetic rule of Moser et al. (1992) at face value it implied that the electron transfer from Mn to Y_Z^{ox} covers a distance of about 1.4 nM in line with our previous results (Mulkidjanian et al. 1996). (2) On $S_2 \Rightarrow S_3$ A_0 was as high as $1.5 \cdot 10^{11}$ s^{-1}. It is thus conceivable that the rate is limited by molecular vibrations. (3) The case $S_4 \rightarrow S_0$ was intermediate, A_0 = $7 \cdot 10^8$ s^{-1}(see 'Discussion' for further details).

The dependence of the rates of electron transfer on the ratio of D_2O over H_2O is shown in Figure 4B. The rates were again determined from transients at 360 nm. On transitions $S_0 \Rightarrow S_1$, $S_1 \Rightarrow S_2$ and $S_4 \rightarrow S_0$ the rates decreased linearly (lines) when progressing from pure H_2O to 98% D_2O (lozenges, triangles, squares). On $S_2 \Rightarrow S_3$ the kinetic isotope effect was again larger than on the other transitions (Table 2). More importantly the data points (Figure 4B, circles) as function of the relative D_2O concentration significantly deviated from a straight line (dashes). Small deuterium concentrations

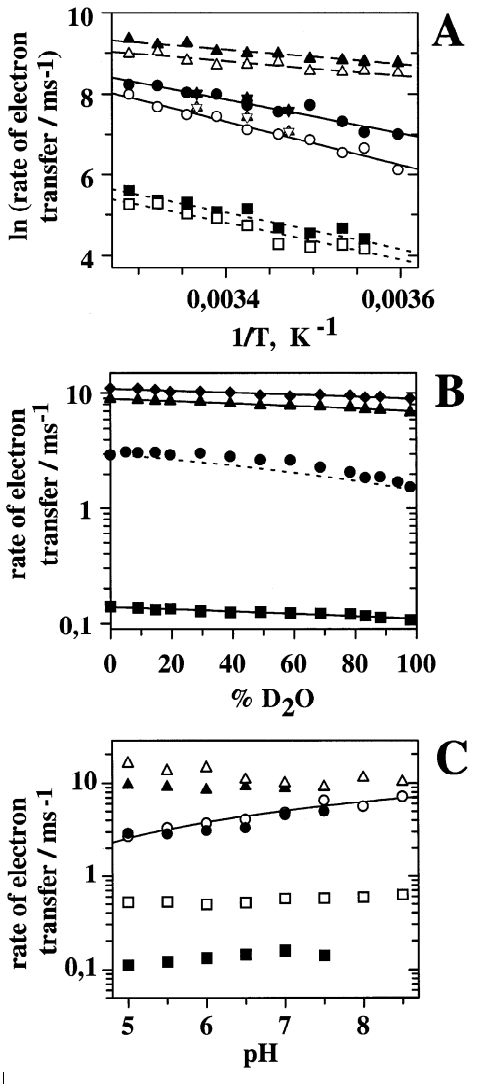

Figure 4. (A) Arrhenius-plot of the rates of electron transfer OEC→Y_Z^{ox} as function of the temperature. The rates were determined from transients at 360 nm as in Figure 3. Solid symbols, H_2O; open symbols, D_2O. Stars give rates as determined from local electrochromism at 443–424 nm on $S_2 \Rightarrow S_3$. For the parameters of the linear regression lines see Table 2. The pL was 6.5. *(B) The rates of electron transfer as function of the D_2O concentration.* The H_2O/D_2O ratio was varied between 100/0 and 2/98%. The steady lines are linear regressions to the data. The dashed line was drawn to illustrate the deviation from linearity on transition $S_2 \Rightarrow S_3$. The temperature was 19 °C, the pL was 6.5. *(C) The rates of electron transfer as function of the pH (in H_2O).* Open symbols, thylakoids; solid symbols, core particles. The line shows the pH-dependence on transition $S_2 \Rightarrow S_3$. The temperature was 19 °C. Symbols: Lozenges, $S_0 \Rightarrow S_1$; triangles, $S_1 \Rightarrow S_2$; circles, $S_2 \Rightarrow S_3$; squares, $S_4 \rightarrow S_0$.

below 40% decreased the rate only weakly. It thus appeared as if the effective deuterium concentration at the site which was responsible for the isotope effect

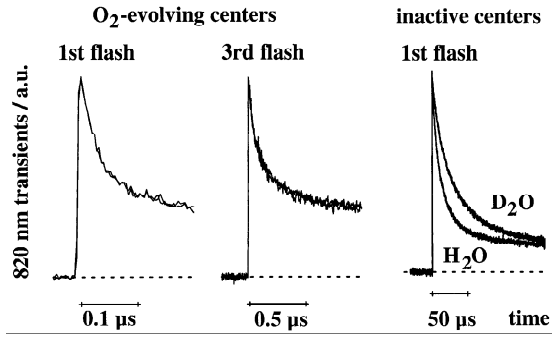

Figure 5. The oxidation/ reduction of P_{680}^+ monitored at 820 nm in PS II core particles in H_2O and D_2O (superimposed). Oxygen evolving material, Left: transients on the first flash, mainly transition $S_1 \Rightarrow S_2$; middle: third flash, mainly $S_3 \Rightarrow S_4$. Inactive material, right: transients on the first flash. Conditions: pL 6.3, chl. 50 μM, hexacyanoferrate(III) 1 mM (plus 0.5 mM hexacyanoferrate(II) in inactive material), DCBQ 0.5 mM, Nd:Yag-laser excitation. Active material: 3 flashes every 30 s, inactive material: 1 flash every 10 s. The time resolution was 4 ns per address, 60 transients were averaged.

was not proportional but lower than the concentration in the medium. A rational for this behaviour is that the proton has a higher affinity to the pertinent binding site than the deuteron (see Bell 1973).

Figure 4C shows the rates of electron transfer at the OEC as function of the pH in H_2O. Open symbols indicate data from thylakoids and solid symbols data from core particles. In agreement with previous reports (Krohs and Metzner 1990; Rappaport et al. 1994) the slow rate on the third flash ($S_4 \rightarrow S_0$, squares) changed only slightly. The half-time decreased from 1.1 ms at pH 8 to 1.35 ms at pH 5. Likewise, the rapid phases on flash no. 1 ($S_1 \Rightarrow S_2$, triangles) revealed little pH dependence. The rate of transition $S_0 \Rightarrow S_1$ was here not determined because of the variation of the Kok-parameters as function of the pH (Lübbers et al. 1993; Haumann and Junge 1994; Bögershausen and Junge 1995a). Only on flash no. 2 ($S_2 \Rightarrow S_3$) a stronger pH dependence was apparent (Figure 4C). The rate varied by a factor of about 2 (see also (Rappaport et al. 1994)). The half-rise times rose from 120 μs (pH 8) to 250 μs (pH 5) both in thylakoids and in core particles.

The pK of acids in contact with D_2O is by about 0.3 units more alkaline than in H_2O (Bell 1973). The rate of electron transfer on $S_2 \Rightarrow S_3$ decreased by a factor of only about 1.3 per pH-unit. According to this rather weak pH-dependence a shift by 0.3 units was expected to decrease the rate only by a factor of 1.1. The observed kinetic isotope effect of about 2 on $S_2 \Rightarrow S_3$ was therefore not attributable to a pK-shift.

We asked for kinetic isotope effects on the reduction of P_{680}^+ by Y_Z. This reaction was followed by absorption transients at 820 nm (see Figure 5). With oxygen evolving core particles (see the two sets of traces in the left of Figure 5) the decay was practically independent of the solvent (H_2O or D_2O). When fitted biexponentially plus an offset the respective half-live times and relative extents were as follows: for the first flash (mainly $S_1 \Rightarrow S_2$) 20 ns (50%), 90 ns (18%), and an offset of 32% both in H_2O and D_2O; on the second flash (mainly $S_3 \Rightarrow S_4$) 30 ns (28%), 150 ns (35%), and an offset of 37%, again both in H_2O and D_2O. These half-times were similar to previously reported ones (Schlodder et al. 1984; van Leeuwen et al. 1992). The absence of a H/D-isotope effect was independent of the incubation time in D_2O ranging from 5 min to 2 h (this work) and from the procedure of lyophilization/D_2O rehydration as applied by Karge et al. (1996). In O_2-evolving centers there was thus no evidence for a steering by protons of the electron transfer from Y_Z to P_{680}^+. This was in line with the results of other authors (Renger et al. 1989; Karge et al. 1996). The situation changed, however, if the Mn-center was inactivated by high pH (see 'Materials and methods'). The respective traces are depicted in the right of Figure 5. The half-decay times of the electron transfer from Y_Z to P_{680}^+ were as follows: 6 μs (61%), 35 μs (26%), and an offset of 13% in H_2O, and 15 μs (61%), 60 μs (26%), and an offset of 13% in D_2O. The average isotope effect was about 2.1 (Table 2).

The abstraction of electrons from the donor side of PS II is transiently accompanied by electrostatically driven proton liberation from peripheral acid groups (Haumann et al. 1994; Bögershausen and Junge 1995b). We determined its average kinetic isotope effect under repetitive flash regime. Figure 6 shows raw transients recorded by the dye bromocresol purple at pL = 6.3 in oxygen-evolving core particles. The dominant (70%) fast component is attributable to proton release from peripheral groups. Its half-rise times were 75 μs in H_2O and 217 μs in D_2O (Figure 6, lines). Their ratio was 2.9 (Table 2). A minor (30%) slow component ($t_{1/2}$ = 750 and 860 μs) was attributable to superimposed protolytic reactions at the PS II acceptor side (Bögershausen and Junge 1995a,b). Its H/D-isotope effect was only 1.15. When the O_2-evolving capacity was inactivated the half-times and the isotope effect of the rapid phase of proton release were the same as in active material.

Table 2. Kinetic H/D isotope effects on the rates of electron transfer, proton release, and oxygen evolution during the catalytic cycle of the oxygen evolving complex in thylakoids and PS II core particles. AH denotes a protonated peripheral amino acid, XH the protonated component X which is oxidized on $S_2 \Rightarrow S_3$

Material	Observable	Transition	Reaction	k_{H2O}/k_{D2O}
Oxygen evolving PS II	Proton release	Average of all	Y_Z+AH→$Y_Z{}^{ox}$+A^-+H^+	2.9
core particles	Electron transfer	$S_0 \Rightarrow S_1$	$MnY_Z{}^{ox} \rightarrow Mn^{ox}Y_Z$	1.3
		$S_1 \Rightarrow S_2$	$P_{680}{}^+Y_Z \rightarrow P_{680}Y_Z{}^{ox}$	1.0
			$MnY_Z{}^{ox} \rightarrow Mn^{ox}Y_Z$	1.3
		$S_2 \Rightarrow S_3$	$XHY_Z{}^{ox} \rightarrow X^{ox}Y_Z + H^+$	2.1
		$S_3 \Rightarrow S_4$	$P_{680}{}^+Y_Z \rightarrow P_{680}Y_Z{}^{ox}$	1.0
		$S_4 \rightarrow S_0$	$(Mn_4X)^{3ox}$ reduction	1.4
Inactive core particles	Proton release		Y_Z+AH→$Y_Z{}^{ox}$+A^-+H^+	2.9
	Electron transfer		$P_{680}{}^+Y_Z \rightarrow P_{680}Y_Z{}^{ox}$	2.1
Thylakoids	Proton release	Average of all	$Y_ZBH \rightarrow Y_Z{}^{ox}\ B^- + H^+$	1.6
	Electron transfer	$S_1 \Rightarrow S_2$	$MnY_Z{}^{ox} \rightarrow Mn^{ox}Y_Z$	1.2
		$S_2 \Rightarrow S_3$	$XHY_Z{}^{ox} \rightarrow X^{ox}Y_Z + H^+$	2.4
		$S_4 \rightarrow S_0$	$(Mn_4X)^{3ox}$ reduction	1.4
	Oxygen liberation		$2H_2O \rightarrow O_2 + 4H^+$	1.4
	Proton release		$2H_2O \rightarrow O_2 + 4H^+$	2.4

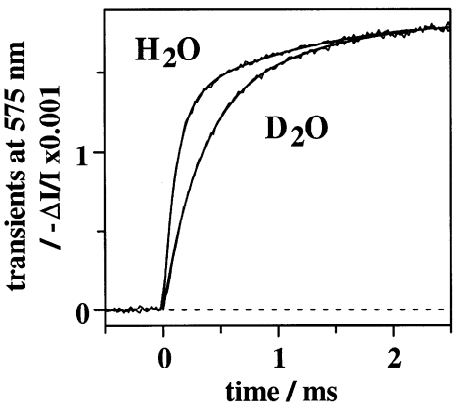

Figure 6. The H/D isotope effect on proton release from peripheral acids in core particles. pH-indicating absorption transients of bromocresol purple at 575 nm were obtained under repetitive flashes at a frequency of 5 Hz in either H_2O or D_2O. 4 μM chlorophyll, 200 μM hexacyanoferrate(III), 100 μM DCBQ, ± dye 30 μM, pL 6.3. 100 transients from 5 independent samples (20 flashes per sample) were averaged, time resolution 20 μs per address, Xenon-flash excitation. The parameters of the lines are shown in Table 2.

H/D-isotope effect of proton release coupled to dioxygen formation from water on $S_4 \rightarrow S_0$

Only in thylakoids but not in core particles proton production during the oxygen evolving step $S_4 \rightarrow S_0$ was kinetically discernible from electrostatically driven proton transfer (Haumann and Junge 1994; Bögershausen and Junge 1995b). Figure 7A shows the characteristic biphasic pH-transient upon the third flash (18 °C, pL 7.4). The rapid rise is owed to an electrostatic response of peripheral amino acids in response to the charge near to $Y_Z{}^{ox}$ and the slower component to 'chemically produced' protons during $S_4 \rightarrow S_0$ (Haumann and Junge 1994). The kinetic isotope effect on the rapid component due to the deprotonation of peripheral acids was 1.6 (Table 2, $t_{1/2}$ = 100 vs. 160 μs). The isotope effect on the rapid phase on the other transitions (not shown) was of similar magnitude. That the isotope effect on the rapid component in thylakoids was smaller than in core particles might indicate the involvement of different peripheral groups with different pKs. The kinetic isotope effect on the slow component, the final chemical production of protons from water (Haumann and Junge 1994), was 2.4 (Table 2, $t_{1/2}$ = 1.3 vs. 2.9 ms). This was significantly larger than the small isotope effect on the rate of electron transfer. Its kinetic isotope effect, as determined from the decays of transients at 360 nm on the third flash (Figure 7B), was 1.4 (Table 2, 1.2 vs. 1.7 ms). The rate of oxygen evolution matched the rate of electron transfer both in H_2O and D_2O (data not shown). Thus, in D_2O, proton release from the final oxidation of water greatly lagged behind electron transfer from water to the OEC (2.9 vs. 1.7 ms). We attributed this lag to the proton transfer reaction itself. This transfer ranged from the site of the chemical production of protons from

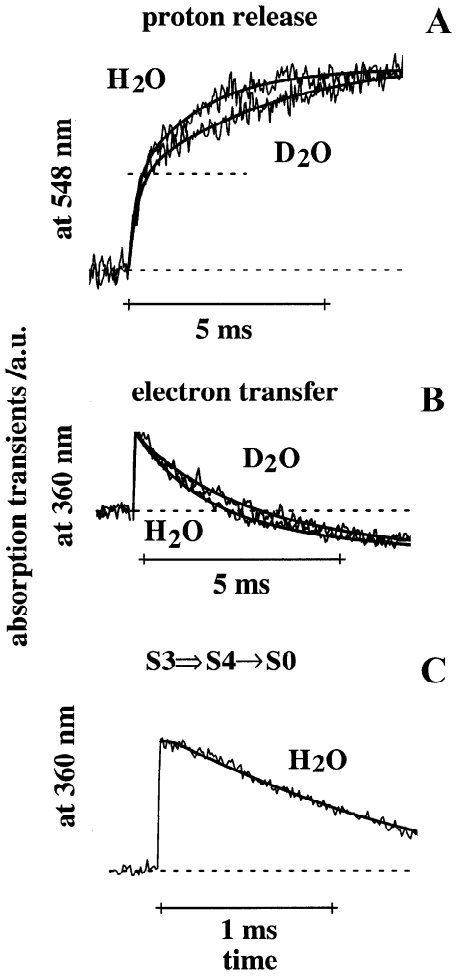

Figure 7. Proton release and electron transfer upon the third flash in dark-adapted thylakoids in H_2O and D_2O. (A) Absorption transients at 548 nm of neutral red (±dye) indicating proton transfer at the lumen side. 200 transients averaged, 2 mM hexacyanoferrate(III) as electron acceptor, pL 7.4. The smooth lines were calculated with the parameters in Table 2. (B) Transients at 360 nm. The decays indicate the reduction of the OEC on $S_4 \rightarrow S_0$. 100 transients averaged, 200 μM hexacyanoferrate(III), 100 μM DCBQ as electron acceptors, pL 7.4. (C) The deconvoluted transient at 360 nm on transition $S_3 \Rightarrow S_4 \rightarrow S_0$ in thylakoids (from Figure 1) shows a time lag. The smooth line was calculated according to Scheme (I) in the text with $k_{-1} = k_2 = 10^4\ s^{-1}$ and $k_{+1} = 10^3\ s^{-1}$. For further details see 'Discussion'.

bound water through the protein to the indicator dye, neutral red, at the lumenal membrane surface. Proton transfer between a neighbouring base and bound water caused a kinetic isotope effect of 1.4 on electron transfer in cytochrome-*c*-oxidase (Hallen and Nilsson 1992) whereas proton transfer from X^{ox} to bulk water caused an effect greater than 2. These results implied that, if electron transfer was limited by proton transfer on transition $S_4 \rightarrow S_0$ at all, this was internal transfer, e.g. between bound water and a buried base. The observable proton release, on the other hand, was kinetically limited by a transfer step that was unrelated to the electron transfer.

We analyzed the kinetics of electron transfer during $S_4 \rightarrow S_0$ in more detail: The UV-transient at 360 nm on the third flash in thylakoids (at pH 6.5, see Figure 1) was composite with relative contributions of transitions $S_0 \Rightarrow S_1$ to $S_3 \Rightarrow S_4 \rightarrow S_0$ of 13: 2: 18: 67% as calculated with Kok-parameters of α/ β/ S_0 of 9/ 8.5/ 5%. We calculated the transients attributable to other transitions than $S_3 \Rightarrow S_4 \rightarrow S_0$ using the half-live times in Table 1. The calculated transients were subtracted from the raw transient on the third flash. This procedure yielded the transient attributable to transition $S_3 \Rightarrow S_4 \rightarrow S_0$. As shown in Figure 7C, it revealed an almost monophasic decay with a half time of 1.3 ms except for a short lag phase, about 100 μs long. A similar lag of UV-transients has been reported previously (Koike et al. 1987; Rappaport et al. 1994). It has also been observed when the decay of Y_Z^{ox} was monitored by EPR (R.J. Pace, personal communication). Rappaport et al. (1994) tentatively attributed this lag to fast proton release, however, without corroborating their proposal by the direct assay of pH-transients. We found that the proton transfer could be even faster than this lag phase depending on the concentration of neutral red in thylakoids (Haumann et al. 1994). This led us to reject the above interpretation and to explain the lag by the consecutive nature of electron transfer from water via manganese/X to Y_Z^{ox}. This is detailed in 'Discussion'. Simulation of consecutive reactions produced the solid line which is shown in Figure 7C.

Discussion

On the chemical nature of the transition $S_2 \Rightarrow S_3$

The component that is oxidized on $S_2 \Rightarrow S_3$ is probably not manganese (Debus 1992; Brudvig 1995). Proposals for the chemical nature of this component range from histidine (His) (Boussac et al. 1990; Ono and Inoue 1992; Boussac and Rutherford 1994; Berthomieu and Boussac 1995; Haumann et al. 1996) over tyrosine Y_Z (Hallahan et al. 1992; Gilchrist et al. 1995) to bound water derivatives (Kusunoki 1995). In Cl^--depleted material we observed that the same component, X, was oxidized on $S_1^* \Rightarrow S_2^*$ as on $S_2 \Rightarrow S_3$ in

controls (Haumann et al. 1995, 1996). The optical difference spectra of the respective transitions were in accord with X being a histidine residue although not proving it (Boussac et al. 1990; Haumann et al. 1996). That the oxidation of X caused the release of one proton into the lumen and that this proton resulted from X^{ox} itself and not from peripheral amino acids (by virtue of their electrostatic response) was supported by three lines of evidence: 1) The rise of the pH-transient revealed a component which kinetically followed the reduction of Y_Z^{ox} by X (Haumann et al. 1995, 1996). (2) A stable electrochromic jump was absent, i.e. X^{ox} was electroneutral (Saygin and Witt 1985, 1987; Haumann et al. 1994; Rappaport et al. 1994), and (3) The kinetic isotope effect on the electron transfer between X and $Y_Z{}^{ox}$ was significantly larger, $\geqslant 2$ (20 °C), as the one of ≤ 1.4 on electron transfer from Mn to $Y_Z{}^{ox}$ and from bound water to Mn_4X (this work). The latter factor is compatible (Bell 1973) with secondary solvent isotope effects and also with the proposed (Krishtalik 1990) binding of OH^- to the OEC on $S_0 \Rightarrow S_1$. The comparatively large kinetic isotope effect on the electron transfer from X to $Y_Z{}^{ox}$ might imply that the rate of this transfer is limited by the protolytic reaction which is coupled to it. A kinetic isotope effect of 2.5 on electron transfer in cytochrome-*c*-oxidase has been attributed to proton transfer between bound water derivatives and bulk water (Hallen and Nilsson 1992). It is thus conceivable that the similarly large effect on electron transfer from X to $Y_Z{}^{ox}$ on $S_2 \Rightarrow S_3$ was caused by the transfer of a proton from X^{ox} to bulk water in the lumen. As a possible clue to the nature of this proton transfer it is worth to recall the predictions of reaction rate theory (Bahnson and Klinman 1995) for proton tunneling, namely a difference of activation energies in D_2O and H_2O of $\Delta Ea \geqslant 5.8$ kJ/mol and a ratio of the preexponential factors of 0.7–0.9. We here report a difference of about 10 kJ/mol and a ratio of 0.8. The rate of electron transfer from X to $Y_Z{}^{ox}$ may therefore be controled by a proton tunneling step.

On the function of Y_Z as a hydrogen acceptor in water oxidation

It has been proposed that $Y_Z{}^{ox}$ may abstract a hydrogen atom from water during the final step of the catalytic cycle, $S_4 \rightarrow S_0$ (Gilchrist et al. 1995; Tommos et al. 1995; Babcock 1995; Hoganson et al. 1995; Britt 1996). This proposal was based on EPR data that have revealed $Y_Z{}^{ox}$ as a neutral radical ($Y_Z{}^{\bullet}$) (Rodriguez et al. 1987; Babcock et al. 1989; Barry et al. 1990). For technical reasons (longevity of the radical) preparations with impaired manganese complex and without oxygen evolving capacity were used in the cited work. If $Y_Z{}^{ox}$ is to act as a hydrogen abstractor, one expects the transient and rapid release of one proton upon its oxidation which occurs during each of the four transitions from $S_0 \Rightarrow S_1$ to $S_3 \Rightarrow S_4$ (Babcock 1995; Hoganson et al. 1995). Such a release has indeed been observed. However, as its extent was variable (as function of the pH and the preparation procedure) and as its rate varied greatly (as function of the buffer concentration and the pH) it has been uneqivocally attributed to an electrostatically induced pK-shift of peripheral amino acids (Lübbers et al. 1993; Lavergne and Junge 1993; Haumann et al. 1994; Haumann and Junge 1994; Bögershausen and Junge 1995b; Haumann and Junge 1996). It was not caused by the chemical production of one proton during the oxidation of Y_Z. This view was corroborated by the observation that the kinetic isotope effect on the reduction of Y_Z^{ox} was variable as function of the S-transition. Another independent line of evidence points into the same direction. $Y_Z{}^{ox}$ is clearly electropositive. Its charge is evident from the rapidly rising ($< 10\ \mu$s) electrochromic transient during each transition from S_0 to S_4 (Haumann et al. 1994, 1996; Rappaport et al. 1994). The subsequent decay of this transient follows with the same rate as electron transfer from the (manganese, X)-entity to $Y_Z{}^{ox}$ (Rappaport et al. 1994; Haumann et al. 1996). The discrepancy between the EPR and the optical spectrophotometric data on $Y_Z{}^{ox}$ seems to be hard. It can be solved, however, by two alternative interpretations: either $Y_Z{}^{ox}$ is only electroneutral in preparations with impaired OEC as used in the cited EPR-work, or $Y_Z{}^{ox}$ is electroneutral *spinwise only and in all materials* but its proton is transfered to and remains on a base B in its close vicinity. In the latter case, $Y_Z{}^{ox}$ has to be conceived as a positively charged entity, namely tyrosine$^{\bullet}$-BH^+ as formed by electron abstraction from tyrosineH-B. That the proton is displaced to a neighbouring base is compatible with the hydrophilic environment (Styring et al. 1993) and the observed hydrogen bonding of the phenol oxygen of Y_Z (Mino and Kawamori 1994; Tommos et al. 1995; Force et al. 1995; Britt et al. 1995; Tang et al. 1996b). The hydrogen bond in the case of Y_Z was found to be less ordered than in the case of Y_D (Britt et al. 1995; Force et al. 1995; Tang et al. 1996b). It should be noted again, however, that these results have been obtained in *inactive* material, i.e. after manganese depletion. That manganese depletion changes the properties of Y_Z has been established (see for example Renger 1979; Con-

jeaud and Mathis 1980; Yuasa et al. 1984). Further evidence for a changed environment comes from the observation that the oxidation of Y_Z by $P_{680}{}^+$ shows a much greater kinetic isotope effect in inactive, e.g. manganese-depleted material than in oxygen evolving centers. If the phenolic proton in inactive material is transferred to a poor acceptor, e.g. to another base or to bulk water, electron transfer from Y_Z to $P_{680}{}^+$ may be rate limited by proton transfer, but only in this material. We consider the extrapolation of data on the hydrogen bond structure of Y_Z from inactive to active material as debatable.

The small kinetic H/D isotope effect on the electron transfer from Y_Z to $P_{680}{}^+$ in active centers (Renger et al. 1989; Karge et al. 1996; this work) makes its steering by the *intra-protein displacement* of the phenolic hydroxyl proton from $Y_Z{}^{ox}$ to B unlikely. The absence of a steering effect requires that proton transfer can be more rapid than electron transfer which may be achieved by the matching of the pKs of the donor ($Y_Z{}^{ox}$) and the accepting base. This will be outlined in more detail in a forthcoming publication. The *observed* rapid deprotonation of peripheral acid groups at the lumenal side upon their coulombic interaction with $Y_Z{}^{\bullet}$-BH^+ (Haumann and Junge 1994; Bögershausen and Junge 1995b) is unrelated to the intra-protein proton displacement to a base B. The former reaction has been characterized as an electrostatically triggered response of peripheral amino acid residues that only negligibly affects the strong electrostatic field in the catalytic center (Haumann and Junge 1994, 1996; Haumann et al. 1994; Bögershausen and Junge 1995b; Mulkidjanian et al. 1996). Consequently, its H/D isotope effect was unrelated to the one of the electron transfer (1.6–2.9 vs. 1.1).

It has been speculated that the rate limiting step on transition $S_4 \rightarrow S_0$ is the abstraction of hydrogen from water by $Y_Z{}^{ox}$ (Gilchrist et al. 1995; Tommos et al. 1995; Babcock 1995). The observed small H/D-isotope effects on electron transfer from Mn_4X to $Y_Z{}^{ox}$ and the above considerations seem to make such a hypothesis less likely. Instead, we consider the deprotonated component X^{ox}, which is possibly His^{ox} and formed on $S_2 \Rightarrow S_3$, as the prime candidate to accept a hydrogen atom during $S_4 \rightarrow S_0$.

Hypothesis on the sequence of events during the oxygen evolving step $S_3 \Rightarrow S_4 \rightarrow S_0$

The electron transfer from water to $(Mn_4XY_Z)^{4ox}$ on $S_4 \rightarrow S_0$ and the release of O_2 showed the same small kinetic isotope effect (1.4) and little pH-dependence which corroborated the notion that these reactions were rate limited by the same kinetic bottleneck (Bouges-Bocquet 1973; Jursinic and Dennenberg 1990). Furthermore, the reduction of $(Mn_4XY_Z)^{4ox}$ by electrons from water on $S_4 \rightarrow S_0$ revealed a lag phase of about 100 μs duration when monitored in the UV (see Rappaport et al. 1994, and Figure 7C) and by EPR (R. Pace, personal communication). In the following we present a model of the sequence of elementary events on $S_4 \rightarrow S_0$ which explains both these phenomena. Our model does not require the sequential binding of the two water molecules mediated by structural changes at the catalytic site as proposed by other authors (Wydrzynski et al. 1996).

It has been proposed from thermodynamic considerations that the most likely pathway to the formation of dioxygen is (i) the rate-limiting two-electron oxidation of two bound water molecules to (bound) hydrogen peroxide which is (ii) rapidly further oxidized to O_2 (Krishtalik 1986, 1990). These events are summarized in a two-step reaction Scheme (I):

$$A \underset{k-1}{\overset{k+1}{\rightleftarrows}} B \xrightarrow{k2} C$$

wherein k_{+1}/k_{-1} denote the forward/reverse rate constants of transient H_2O_2 formation and k_2 the rate of the slowest among the two subsequent one-electron reactions. We further define the equilibrium constant of peroxide formation by $K_1 = k_{+1}/k_{-1}$. The state *A* is identified with $S_4 = (H_2O)_2(Mn_4X)^{3ox}Y_Z{}^{ox}$ or $S_3Y_Z{}^{ox}$ in terms of Kok's nomenclature. Water is most probably bound to the Mn-cluster. Thus, we assign the state *B* to $(H_2O_2{+}2H^+)(Mn_4X)^{1ox}Y_Z{}^{ox}$. The formation of *C* is equivalent to the reduction of $(Mn_4X)^{1ox}$ and $Y_Z{}^{ox}$. We denote the initial concentrations of *A* and *B* after the oxidation in nanoseconds of Y_Z on $S_3 \Rightarrow S_4$ as A_0 and B_0,

$$A_0 = \frac{1}{1+K_1}, \quad B_0 = \frac{K_1}{1+K_1} \tag{2}$$

When assuming (pseudo-) first order reactions the solution of the kinetic scheme (I) reveals bi-exponential behaviour:

$$B(t) = B_1 \cdot \mathrm{e}^{-\lambda_1 t} - B_2 \cdot \mathrm{e}^{-\lambda_2 t} \tag{3}$$

$$C(t) = 1 - C_1 \cdot \mathrm{e}^{-\lambda_1 t} - C_2 \cdot \mathrm{e}^{-\lambda_2 t} \tag{4}$$

wherein λ_1, λ_2, B_1, B_2, C_1 and C_2 are as follows:

$$\lambda_{1,2} = 0.5 \cdot (k_{+1} + k_{-1} + k_2 \mp \sqrt{(k_{+1} + k_{-1} + k_2)^2 - 4 \cdot k_{+1} \cdot k_2}),$$

$$B_1 = \frac{\lambda_1}{k_2} \cdot \frac{\lambda_2 - \frac{K_1}{1+K_1} \cdot k_2}{\lambda_2 - \lambda_1}, \quad B_2 = B_1 - \frac{K_1}{1 + K_1},$$

$$C_1 = \frac{\lambda_2 - \frac{K_1}{1+K_1} \cdot k_2}{\lambda_2 - \lambda_1}, \quad C_2 = 1 - C_1 \qquad (5)$$

A lag phase of the appearance of *C*, of similar magnitude as documented in Figure 7C implies an equilibrium constant $K_1 \geqslant 0.1$ or a change in free energy upon peroxide formation of only $\leqslant$ +60 mV. In state S_4 the equilibrium between bound peroxide and bound water might be poised towards water, even more so in S_3. This may be why the two bound water molecules are exchangable with time constants of 30 and 500 ms (Messinger et al. 1995) in state S_3. Thus the state S_3 is conceived as $(H_2O)_2(Mn_4X)^{3ox}$ with a minor admixture of $(H_2O_2{+}2H^+)(Mn4X)^{1ox}$. The deposition of one further electron on $(Mn_4X)^{1ox}$ in S_3 is energetically unfavorable as the midpoint potential of the respective redox couple, which is probably equivalent to S_1/S_0, is too low. This explains the stability of S_3 as compared with S_4. It should be noted that we consider the proposed *release* of peroxide by PS II (e.g. in inactive centers) (Wydrzynski et al. 1996) as unlikely unless the free energy of the oxidation of a donor (i.e. a reduced electron acceptor molecule) is coupled to the reaction. Only after the formation of $Y_Z{}^{ox}$ in S_4 two further electron holes are available which provides the driving force to oxidize peroxide to dioxygen (right hand side of Scheme (I)). The additional positive charge on $Y_Z{}^{ox}$ (equivalent to $Y_Z{}^{\bullet}$-BH^+) in state S_4 may shift the equilibrium between water and peroxide to the right (increase the equilibrium constant) by elevating the midpoint potential of $(Mn_4X)^{3ox}$ *relative* to the one of bound water by coulombic interaction. The distance between bound water and Mn may be taken as 0.3–0.5 nm, and the effective dielectric permittivity as 10 (Mulkidjanian et al. 1996). A distance between Mn and Y_Z of about 1.5 nm is compatible with data of local electrochromic bandshifts (Mulkidjanian et al. 1996) and pulsed EPR (Kodera et al. 1995; Hara et al. 1996, the latter results were also compatible with the placement of the component X at a distance of about 0.6 nm from Y_Z, about halfway to Mn). Taking these results together, the potential of $(Mn_4X)^{3ox}$ *relative* to the one of bound water increases by about 50 mV by the charge on $Y_Z{}^{ox}$. Thus, for the two electron process of peroxide formation the change in free energy may be decreased by as much as 100 mV which corresponds to an increase of the equilibrium constant between water and peroxide in state S_4 (K_1) with respect to state S_3 by about two orders of magnitude.

Table 3. The Arrhenius activation parameters of electron transfer at the OEC in PS II core particles. The uncertainties in the activation energies were on the order of $\pm$ 2 kJ/mol

Transition	Medium	Activation energy, E_a, kJmol^{-1}	Preexponential factor, ln A_0
$S_1 \Rightarrow S_2$	H_2O	14.6	15.0
	D_2O	14.6	14.8
$S_2 \Rightarrow S_3$	H_2O	35.0	22.1
	D_2O	45.0	25.7
$S_4 \rightarrow S_0$	H_2O	37.5	20.4
	D_2O	37.5	20.1

The above considerations were applied to the observed UV-transient of $(Mn_4XY_Z)^{4ox}$ reduction on $S_4 \rightarrow S_0$ as documented in Figure 7C. The transient was well described by Scheme (I) with the following rate constants: $k_{+1} = 10^3$ s^{-1}, $k_{-1} = 10^4$ s^{-1}, and $k_2 = 10^4$ s^{-1} (smooth line). The magnitude of the rate constant k_2 (10^4 s^{-1}) was similar to the rate of the transition $S_1 \Rightarrow S_2$. We conclude that the second step of Scheme (I) reflects the same reaction as on $S_1 \Rightarrow S_2$, namely the oxidation of $(MnX)^{1ox}$ by $Y_Z{}^{ox}$. The latter reaction is characterized by an activation energy of about 15 kJmol^{-1} and a preexponential factor of $3 \cdot 10^6$ s^{-1} (see Table 3). The formation of peroxide on the first step of Scheme (I) is probably accompanied by essential nuclear and electronic reorganizations of the Mn cluster. Indeed, the rate of electron transfer rate on $S_4 \rightarrow S_0$ decreased by a factor of 4 in core particles, whereas the rates during the other transitions were about the same as in thylakoids. On these grounds one would expect a higher activation energy for the reactions k_{+1} and k_{-1} and, thus, their temperature dependence to be steeper than the one of k_2. The rate of the whole process described by Scheme (I) is approximated by:

$$k = \frac{k_{+1} \cdot k_2}{k_{-1} + k_2} \qquad (6)$$

Thus, at high temperatures the rate of oxygen evolution will be determined by

$$k = \frac{k_{+1} \cdot k_2}{k_{-1}} \qquad (7)$$

whereas at low temperatures by

$$k = k_{+1} \qquad (8)$$

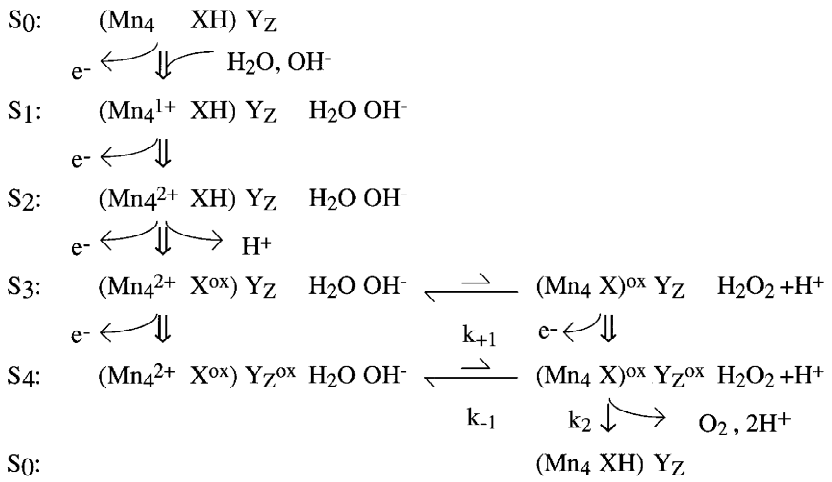

Scheme II . A tentative reaction scheme of the electron transfer reactions in the Kok-cycle. The light driven reactions of electron abstraction are denoted by 'e^-'. $S_0 \Rightarrow S_1$: Mn^{II} is oxidized to Mn^{III}, the binding of OH^- to Mn keeps this transition electroneutral, the entry of the second water molecule is optional; $S_1 \Rightarrow S_2$: Mn^{III} is oxidized to Mn^{IV}, one surplus charge remains in the center; $S_2 \Rightarrow S_3$: X is oxidized and deprotonated, bound water and peroxide are in equilibrium in the S_3-state, but poised towards bound water as indicated by the arrow lengths; $S_3 \Rightarrow S_4$: Y_Z^{ox} is formed by P_{680}^+; $S_4 \rightarrow S_0$: Oxygen is evolved in a sequential two step mechanism, with peroxide as an obligatory intermediate; for further details see Scheme (I) and text.

This implies a different slope in an Arrhenius plot of the rates of oxygen evolution at low and at high temperatures. The activation energy of oxygen evolution in the high-temperature limit is the sum of ΔG_1 and the activation energy of transition $S_1 \Rightarrow S_2$. This sum calculates to about 20 kJ/mol which is similar to the figures in the literature (Renger et al. 1989; Renger and Hanssum 1992). In the low-temperature region, the activation energy should be essentially higher. An increased activation energy of about 46–60 $kJmol^{-1}$ at low temperatures has indeed been observed (Renger et al. 1989; Renger and Hanssum 1992).

Conclusions

The oxidation of the component X during $S_2 \Rightarrow S_3$ revealed a greater kinetic isotope effect (2.1–2.4) and a larger pH-dependence than all other transitions both in thylakoids and PS II core particles: It is likely that the electroneutral electron transfer $X \rightarrow Y_Z^{ox}$ is kinetically controlled by proton extrusion from X^{ox}(His^{ox}?) into bulk water. On the basis of our data on electron transfer, on proton release, and on local electrochromism we conclude that Y_Z^{ox} is truly $Y_Z^{\bullet}$-BH^+ wherein B denotes a base in the vicinity of Y_Z. The electron transfer from Y_Z to P_{680}^+ is not rate limited by proton transfer from Y_Z-OH to the base B. $Y_Z^{\bullet}$-BH^+ is inappropriate to act as a hydrogen acceptor from bound water. X^{ox}, on the other hand, is a possible candidate for accepting a hydrogen atom from water during the oxygen evolving step $S_4 \rightarrow S_0$. This hydrogen transfer may facilitate electron transfer during the final steps of water oxidation.

The oxygen evolving transition $S_4 \rightarrow S_0$ revealed only a small kinetic isotope effect and the corresponding pH-transient was kinetically uncorrelated with electron transfer. We propose that transition $S_4 \rightarrow S_0$ is rate limited by the first out of two two-electron transfer steps from bound water to the oxidized Mn_4X-entity which leads to the intermediate formation of bound peroxide. Peroxide oxidation is probably rapid and only rate limited by electron transfer from Mn_4X to Y_Z^{ox}. These reactions are summarized in Scheme (II).

Acknowledgements

The authors thank H. Kenneweg for excellent technical assistance. Financial support from the Deutsche Forschungsgemeinschaft (SFB171/A2), the Fonds der Chemischen Industrie, and from INTAS (INTAS-93-2852) is gratefully acknowledged.

References

Allakhverdiev SI, Klimov VV and Demeter S (1992) Thermoluminescence evidence for light-induced oxidation of tyrosine and histidine residues in manganese-depleted Photosystem-II particles. FEBS Lett 297(1,2): 51–54

Babcock GT (1995) The oxygen evolving complex of Photosystem II as a metallo radical enzyme. In: Mathis P (ed) Photosynthesis: From Light to Biosphere, Vol 2, pp 209–215. Kluwer Academic Publishers, Dordrecht

Babcock GT, Blankenship RE and Sauer K (1976) Reaction kinetics for positive charge accumulation on the water side of chloroplast Photosystem II. FEBS Lett 61(2): 286–289

Babcock GT, Barry BA, Debus RJ, Hoganson CW, Atamian M, McIntosh L, Sithole U and Yocum CF (1989) Water oxidation in Photosystem II: From radical chemistry to multielectron chemistry. Biochemistry 28: 9557–9565

Bahnson BJ and Klinman JP (1995) Hydrogen tunneling in enzyme catalysis. In: Purich LD (ed) Methods in Enzymology, pp 373–397. Academic Press, New York

Barry BA, El-Deeb MK, Sandusky PO and Babcock GT (1990) Tyrosine radicals inPhotosystem II and related model compounds. J Biol Chem 265(33): 20139–20143

Bell RP (1973) The Proton in Chemistry. Chapman and Hall, London

Berthomieu C and Boussac A (1995) Histidine oxidation in the S-2 to S-3 transition probed by FTIR difference spectroscopy in the Ca2+-depleted Photosystem II – comparison with histidine radicals generated by UV irradiation. Biochemistry 34: 1541–1548

Bögershausen O and Junge W (1995a) Protolytic reactions at the donor and the acceptor side of Photosystem II core particles. In: Mathis P (ed) Photosynthesis: From Light to Biophere Vol 2, pp 263–266. Kluwer Academic Publishers, Dordrecht

Bögershausen O and Junge W (1995b) Rapid proton transfer under flashing light at both functional sides of dark adapted Photosystem II core particles. Biochim Biophys Acta 1230: 177–185

Bouges-Bocquet B (1973) Limiting steps in Photosystem II and water decomposition in Chlorella and Spinach chloroplasts. Biochim Biophys Acta 292: 772–785

Boussac A and Rutherford AW (1994) Electron transfer events in chloride-depleted Photosystem II. J Biol Chem 269: 12462–12467

Boussac A, Zimmermann JL, Rutherford AW and Lavergne J (1990) Histidine oxidation inthe oxygen-evolving Photosystem-II enzyme. Nature 347: 303–306

Britt RD (1996) Oxygen evolution. In: Ort D and Yocum CF (eds) Oxygenic Photosynthesis: The Light Reactions, pp 137–164. Kluwer Academic Publishers, Dordrecht

Britt RD, Randall DW, Ball JA, Gilchrist ML, Force DA, Sturgeon BE, Lorigan GA, Tang XS et al. (1995) Electron spin echo – endor studies of the tyrosine radicals and the manganese cluster of Photosystem II. In: Mathis P (ed) Photosynthesis: From Light to Biosphere, Vol 2, pp 223–228. Kluwer Academic Publishers, Dordrecht

Brudvig GW (1995) Structure and function of manganese in Photosystem II. Adv Chem Ser 246: 249–263

Conjeaud H and Mathis P (1980) The Effect of pH on the reduction kinetics of *P*-680 in Tris-treated chloroplasts. Biochim Biophys Acta 590: 353–359

Debus RJ (1992) The manganese and calcium ions of photosynthetic oxygen evolution. Biochim Biophys Acta 1102: 269–352

Dekker JP, Plijter JJ, Ouwenand L and Van Gorkom HJ (1984) Kinetics of manganese redox transitions in the oxygen evolving apparatus of photosynthesis. Biochim Biophys Acta 767: 176–179

Force DA, Randall DW, Britt RD, Tang XS and Diner BA (1995) 2H ESE-ENDOR study of hydrogen bonding to the tyrosine radicals YD° and YZ° of Photosystem II. J Am Chem Soc 117: 12643–12644

Ghanotakis DF, Demetriou DM and Yocum CF (1987) Isolation and characterization of an oxygen-evolving Photosystem II reaction center core preparation and a 28 kDa chl-*a*-binding protein. Biochim Biophys Acta 891: 15–21

Gilchrist ML,Ball JA,Randall DW and Britt RD (1995) Proximity of the manganese cluster of Photosystem II to the redox-active tyrosine Y-Z. Proc Natl Acad Sci USA 92: 9545–9549

Hallahan BJ, Nugent JHA, Warden JT and Evans MCW (1992) Investigation of the origin of the 'S3' EPR signal from the oxygen-evolving complex of Photosystem 2: The role of tyrosine Z. Biochemistry 31: 4562–4573

Hallen S and Nilsson T (1992) Proton transfer during the reaction between fully reduced cytochrome *c* oxidase and dioxygen: pH and deuterium isotope effects. Biochemistry 31: 11853–11859

Hara H, Kawamori A, Astashkin AV and Ono T (1996) The distances from tyrosine D to redox active components on the donor side of Photosystem II determined by pulsed electron paramagnetic resonance. Biochim Biophys Acta 1276: 140–146

Haumann M and Junge W (1994) Extent and rate of proton release by photosynthetic wateroxidation in thylakoids: Electrostatic relaxation versus chemical production. Biochemistry 33: 864–872

Haumann M and Junge W (1996) Protons and charge indicators in oxygen evolution. In: Ort D and Yocum CF (eds) Advances in Photosynthesis: Oxygenic Photosynthesis – The Light Reactions, pp 137–164. Kluwer Academic Publishers, Dordrecht

Haumann M, Bögershausen O and Junge W (1994) Photosynthetic oxygen evolution: Net charge transients as inferred from electrochromic bandshifts are independent of protonrelease into the medium. FEBS Lett 355: 101–105

Haumann M, Hundelt M, Drevenstedt W and Junge W (1995) Electrogenicity of electron andproton tranfer in Photosystem II of green plants. In: Mathis P (ed) Photosynthesis: From Light to Biosphere, pp 333–336. Kluwer Academic Publishers, Dordrecht

Haumann M, Drevenstedt W, Hundelt M and Junge W (1996) Photosystem II of green plants. Oxidation and deprotonation of the same component (histidine?) on $S_1^* => S_2^*$ in chloride-depleted centers as on $S_2 => S_3$ in controls. Biochim Biophys Acta 1273: 237–250

Hoganson CW, Lydakis-Simantiris N, Tang XS, Tommos C, Warncke K, Babcock GT, Diner BA, McCracken J and Styring S (1995) A hydrogen-atom abstraction model for the function of Yz in photosynthetic oxygen evolution. Photosynth Res 46: 177–184

Junge W (1976) Flash kinetic spectrophotometry in the study of plant pigments. In: Goodwin TW (ed) Chemistry and Biochemistry of Plant Pigments, pp 233–333. Academic Press, New York

Jursinic P and Dennenberg RJ (1990) Oxygen release time in leaf discs and thylakoids of peas and Photosystem II membrane fragments of spinach. Biochim Biophys Acta 1020: 195–206

Karge M, Irrgang K-D, Sellin S, Feinaeugle R, Liu B, Eckert H-J, Eichler HJ and Renger G (1996) Effects of hydrogen/deuterium exchange on photosynthetic water cleavage in PS II core complexes from spinach. FEBS Lett 378: 140–144

Klein MP, Sauer K and Yachandra VK (1993) Perspectives on the structure of thephotosynthetic oxygen evolving manganese complex and its relation to the Kok cycle. Photosynth Res 38: 265–277

Kodera Y, Hara H, Astashkin AV, Kawamori A and Ono T (1995) EPR study of trapped Z+ in Ca-depleted Photosystem II. Biochim Biophys Acta 1232: 43–51

Koike H, Hanssum B, Inoue Y and Renger G (1987) Temperature dependence of S-state transition in a thermophilic cyanobacterium, *Synechococcus vulcanus* Copeland measured by absorption changes in the ultraviolet region. Biochim Biophys Acta 893: 524–533

Krishtalik LI (1986) Energetics of multielectron reactions. Photosynthetic oxygen evolution. Biochim Biophys Acta 849: 162–171

Krishtalik LI (1990) Activation energy of photosynthetic oxygen evolution: An attempt at theoretical analysis. Bioelectrochem Bioenerg 23: 249–263

Krohs U and Metzner H (1990) Overall kinetics of Photosystem II: pH dependence anddeuterium isotope effect. Bioelectrochem Bioenerg 23: 141–152

Kusunoki M (1995) EPR evidence for the primary water oxidation step upon the $S_2$to S_3 transition in the Joliot-Kok cycle of plant Photosystem II. Chem Phys Lett 239: 148–157

Lavergne J and Junge W (1993) Proton release during the redox cycle of the water oxidase. Photosynth Res 38: 279–296

Lübbers K, Haumann M and Junge W (1993) Photosynthetic water oxidation under flashing light. Oxygen release, proton release and absorption transients in the near UV – a comparison between thylakoids and a reaction-center core preparation. Biochim Biophys Acta 1183: 210–214

Lydakis-Simantiris N, Hoganson CW, Ghanotakis DF and Babcock GT (1995) Deuteriumisotope effects on the kinetics of Yzdeg reduction in oxygen evolving Photosystem II membranes. In: Mathis P (ed) Photosynthesis: From Light to Biosphere, Vol 2, pp 279–282. Kluwer Academic Publishers, Dordrecht

Messinger J, Badger M and Wydrzynski T (1995) Detection of one slowly exchanging substrate water molecule in the S3 state of Photosystem II. Proc Natl Acad Sci USA 92: 3209–3213

Mino H and Kawamori A (1994) Microenvironments of tyrosine D^+ and tyrosine Z^+ in Photosystem II studied by proton matrix ENDOR. Biochim Biophys Acta 1185: 213–220

Moser CC, Keske JM, Warncke K, Farid RS and Dutton PL (1992) Nature of biological electron transfer. Nature 355: 796–802

Mulkidjanian AY, Cherepanov DA, Haumann M and Junge W (1996) Photosystem II of green plants: Topology of core pigments and redox cofactors as inferred from electrochromic difference spectra. Biochemistry 35: 3093–3107

Ono T and Inoue Y (1991) A possible role of redox-active histidine in the photoligation of manganese into a photosynthetic O_2-evolving enzyme. Biochemistry 30: 6183–6188

Ono T and Inoue Y (1992) Localization in Photosystem II of the histidine residue putatively responsible for thermoluminescence A_t-band as probed by trypsin accessibility. Biochim Biophys Acta 1099: 185–192

Ono T, Nogushi T, Inoue Y, Kusunoki M, Matsushita T and Oyanagi H (1992) X-ray detection of the period-four cycling of the manganese cluster in photosynthetic wateroxidizing enzyme. Science 258: 1335–1337

Ono T, Noguchi T, Inoue Y, Kusunoki M, Yamaguchi H and Oyanagi H (1995) XANES spectroscopy for monitoring intermediate reaction states of Cl^--depleted Mn cluster in photosynthetic water oxidation enzyme. J Am Chem Soc 117: 6386–6387

Rappaport F, Blanchard-Desce M and Lavergne J (1994) Kinetics of electron transfer andelectrochromic change during the redox transition of the photosynthetic oxygen-evolving complex. Biochim Biophys Acta 1184: 178–192

Renger G (1979) A rapid vectorial back reaction at the reaction centers of Photosystem II in Tris-washed chloroplasts induced by repetitive flash excitation. Biochim Biophys Acta 547: 103–116

Renger G and Hanssum B (1992) Studies on the reaction coordinates of the water oxidase in PS II membrane fragments from spinach. FEBS Lett 299: 28–32

Renger G and Weiss W (1986) Studies on the nature of the water oxidizing enzyme. III. Spectral characterization of the intermediary redox states in the water-oxidizing enzyme system Y. Biochim Biophys Acta 850: 184–196

Renger G, Eckert HJ, Hagemann R, Hanssum B, Koike K and Wacker U (1989) New results on the mechanism of photosynthetic water oxidation. In: Singhal GS, Barber J, Dilley RA, Govindjee, Haselkorn R and Mohanty P (eds) Photosynthesis: Molecular Biology and Bioenergetics, pp 357–371. Narosa Publ. House, New Delhi

Renger G, Bittner T and Messinger J (1994) Biochem Soc Trans 22: 318–322

Rodriguez ID, Chandrashekar TK and Babcock GT (1987) Endor characterization of H2O/D2O exchange in the D+Z+ radical in photosynthesis. In: Biggins J (ed) Progress in Photosynthesis Research, pp 471–475. Martinus Nijhoff Publishers, Dordrecht

Roelofs TA, Ling W, Latimer, MJ, Cinco RM, Rompel A, Andrews JK, Sauer, K, Yachandra VK and Klein M (1996) Oxidation states of the manganese cluster during the flash-induced S-state cycle of the photosynthetic oxygen-evolving complex. Proc Natl Acad Sci USA 93(8): 3335–3340

Saygin Ö and Witt HT (1985) Sequence of the redox changes of manganese and pattern of the changes of charges during water cleavage in photosynthesis. Photobiochem Photobiophys 10: 71–82

Saygin Ö and Witt HT (1987) Optical characterization of intermediates in the water-splitting enzyme system of photosynthesis – possible states and configurations of manganese and water. Biochim Biophys Acta 893: 452–469

Schlodder E, Brettel K, Schatz GH and Witt HT (1984) Analysis of the Chl-$a_{II}{}^+$ reduction kinetics with nanosecond time resolution in oxygen-evolving Photosystem II particles from *Synechococcus* at 680 and 824 nm. Biochim Biophys Acta 765: 178–185

Sinclair J and Arnason T (1974) Studies on a thermal reaction associated with photosynthetic oxygen evolution. Biochim Biophys Acta 368: 393–400

Styring S, Davidsson L, Tommos C, Vermaas WFJ, Vass I and Svensson B (1993) Structureof redox components in Photosystem 2 studied with computer modeling, site-directed mutagenesis and EPR spectroscopy. Photosynthetica 28: 225–241

Tang XS, Randall DW, Force BA, Diner BA and Britt RD (1996a) Manganese-tyrosineinteraction in the Photosystem II oxygen evolving complex. J Am Chem Soc 118(32): 7638–7639

Tang XS, Zheng M, Chisholm DA, Dismukes GC and Diner BA (1996b) Investigation of the differences in the local protein environments surrounding tyrosine radicals YZ and YD in Photosystem II using wild-type and the D2-Tyr160Phe mutant of Synechocystis 6803. Biochemistry 35: 1475–1484

Tommos C, Tang XS, Warncke K, Hoganson CW, Styring S, McCracken J, Diner BA andBabcock GT (1995) Spin-density distribution, conformation and hydrogen bonding of the redox-active tyrosine YZ in Photosystem II from multiple electron magnetic-resonance spectroscopies: Implications for photosynthetic oxygen evolution. J Am Chem Soc 117: 10325–10335

Trissl HW, Breton J, Deprez J and Leibl W (1987) Biochim Biophys Acta 893: 305–319

van Leeuwen PJ, Heimann C, Kleinherenbrink FAM and van Gorkom HJ (1992) Kinetics of electron transport on the donor

side of spinach photosystem core particles. In: Murata N (ed) Research in Photosynthesis, Vol 2, pp 341–344. Kluwer Academic Publishers, Dordrecht

van Leeuwen PJ, Nieveen MC, van de Meent EJ, Dekker JP and Van Gorkom HJ (1991) Rapid and simple isolation of pure Photosystem II core and reaction center particles from spinach. Photosynth Res 28: 149–153

Velthuys BR (1988) Spectroscopic characterization of the acceptor state Qa- and the donor state S2 of Photosystem II of spinach in the blue, red and near-infrared. Biochim Biophys Acta 933: 249–257

Wydrzynski T, Hillier W and Messinger, J (1996) On the functional significance of substrate water accessibility in the photosynthetic water oxidation mechanism. Physiol Plant 96(2): 342–350

Yuasa M, Ono T and Inoue Y (1984) Isolation of Photosystem II reaction center complexretaining 33 kDa protein and Mn, a possible structural minimum of photosynthetic O_2-evolving system. Photobiochem Photobiophys 7: 257–266